www.czasopisma.pan.pl PAN POLSKA AKADEMIA NAUK www.journals.pan.pl

A R C H I V E S O F M E T A L L U R G Y A N D M A T E R I A L S

Volume 60 2015 Issue 3

DOI: 10.1515/amm-2015-0304

K. DUDEK*,# T. GORYCZKA*, T. WIERZCHOŃ**, J. LELĄTKO*

STRUCTURE OF TiN/HYDROXYAPATITE MULTILAYERS DEPOSITED ON SURFACE OF NiTi SHAPE MEMORY ALLOY

STRUKTURA WARSTW TiN/HYDROKSYAPATYT WYTWORZONYCH NA POWIERZCHNI STOPÓW NiTi WYKAZUJĄCYCH EFEKT PAMIĘCI KSZTAŁTU

In order to improve a corrosion resistance and biocompatibility of NiTi shape memory alloys, the surface of the NiTi alloy was covered by protective layers. The paper presents results of the layers composed of titanium nitride and hydroxyapatite (HAp). The TiN layers were deposited using the glow discharge technique and then the bioactive hydroxyapatite layer was formed from simulated body fluids solution. The results of the structure studies and microscopic observations confirmed that on the surface of the NiTi alloy a thin titanium nitride layer 35-50 nm thick (depending on the glow discharge technique parameters) was obtained. The structure of the deposited layers was studied by means of the X-ray diffraction technique. Also, mechanical parameters of obtained layers were characterized using nanoindentation. On the top of the titanium nitride, a layer consisted of hydroxyapatite and NaCl was formed. Applied parameters of deposition process did not lead to decomposition of the NiTi parent phase (B2) to the equilibrium ones.

Keywords: NiTi, surface modification, glow discharge technique, TiN, hydroxyapatite.

W celu poprawy właściwości korozyjnych, biokompatybilności oraz biofunkcjonalności stopów NiTi wykazujących efekt pamięci kształtu, stosuje się różne metody modyfikacji ich powierzchni. W prezentowanej pracy przedstawiono wyniki badań warstw powierzchniowych złożonych z azotków tytanu oraz hydroksyapatytu. Warstwy TiN zostały wytworzone przy użyciu metody jarzeniowej, a następnie na ich powierzchni został osadzony hydroksyapatyt z roztworu SBF. Wyniki przeprowadzonych badań strukturalnych oraz obserwacji mikroskopowych potwierdziły, że na powierzchni stopu NiTi wytworzyła się cienka warstwa azotku tytanu o grubości 35-50 nm (w zależności od zastosowanych parametrów procesu jarzeniowego). Z kolei na powierzchni warstwy azotowanej powstała warstwa składająca się z hydroksyapatytu oraz NaCl. Zastosowane parametry wytwarzania warstw nie doprowadziły do rozkładu fazy macierzystej stopu NiTi (B2) na fazy równowagowe. Fakt ten jest niezwykle istotny z uwagi na wystąpienie odwracalnej przemiany martenzytycznej oraz zjawiska pamięci kształtu.

1. Introduction

NiTi alloys with chemical composition close to equiatomic reveal very good mechanical properties, high corrosion resistance, biocompatibility and unique features such as shape memory and superelasticity effects. The NiTi alloys have been increasingly used in a wide range of biomedical fields such as implants in orthopedic, for cardiovascular applications, dental application, in soft tissue surgery as well as a part of medical devices. Nevertheless, the applications of the NiTi shape memory alloy, especially as long-term implants, can be limited.

The source of the limitation is a possibility of nickel ion migration into a human body. In consequence of that corrosion of the alloy could be take toxic effect on the patient's body [1, 2].

In order to improve the corrosion resistance of the NiTi alloys, its surface can be modified by formation of multifunctional protective layers [3-6]. The surface modification with use of apatite coatings may additionally enhances biocompatibility and osteoconductivity of the implants [7-9].

Most of the deposition processes frequently used for surface modification require increase of temperature. In case of NiTi shape memory alloys it can lead to decomposition of the B2 phase to equilibrium ones (Ni3Ti and/or NiTi2). In consequence of that the shape memory effect (SME) and superelasticity (SE) can be damaged. Also, the SME may be limited by too thick and/or too stiff coatings.

Taking into account all these advantages, requirements and limitations, the surface of the NiTi alloy was modified with deposition of multilayer consisted of titanium nitride as well as hydroxyapatite (HAp). In the present paper structure as well as mechanical properties of TiN/HAp multilayer is discussed.

* UNIVERSITY OF SILESIA, INSTITUTE OF MATERIALS SCIENCE, , 1A 75 PUŁKU PIECHOTY, 41-500 CHORZÓW, POLAND

** WARSAW UNIVERSITY OF TECHNOLOGY, FACULTY OF MATERIALS SCIENCE AND ENGINEERING, 141 WOŁOWSKA STR., 02-507 WARSZAWA, POLAND

Corresponding author: kdudek@us.edu.pl

2. Experimental procedure

The commercial NiTi alloy with nominal chemical composition 50.6 at.% Ni and 49.4 at. % Ti was used as a substrate for layers deposition. The rectangular samples of the alloy with dimension of 10 mm x 8 mm x 0.8 mm were cut from the NiTi sheet. Next, the samples were polished with SiC papers down to 1200 grit, diamond suspensions up to 1 μm and finally 0.1 μm colloidal silica suspension.

First, the surface of the NiTi alloy was nitrided using glow discharge technique at low temperature: 250°C and 300°C and deposition time 15 min. or 30 min., respectively. In order to deposit the hydroxyapatite layers on the top of the nitrided samples they were immersed in Hank's solution for 7 days. The chemical composition of the solution can be find elsewhere [7]. After that coatings were dried at the room temperature.

The structure of the coated NiTi alloy was investigated by means of the X-ray grazing incidence diffraction (GIXRD). The GIXRD patterns were measured at constant incidence angle of 0.2, 0.3, 0.5 and 1.0° at room temperature using X-ray diffractometer X'PertPro with monochromatized Cu Kα radiation. The X-ray diffraction patterns were measured in the 2theta range of 20-85 degrees. The thickness, surface roughness, interface roughness and density of the nitride layers and metal matrix were calculated from X-ray reflectivity measurement.

The surface of the coated samples was observed using a JEOL JSM-6480 scanning electron microcope (SEM) equipped with Energy Dispersive Spectometer (EDS) enabling a analysis of chemical composition.

The mechanical parameters such as hardness and Young's modulus of obtained layers were studied using Hysitron Triboindenter TI- 950.

3. Results and discussion

NiTi surface after nitriding

Phase identification of the layers formed, on NiTi surface, after nitriding was determined by X-ray diffraction patterns measured at room temperature. Figure 1 shows the set of GIXRD patterns for the sample nitrided at 300°C for 30 min. The diffraction lines belonging to substrate - the parent phase B2 - were identified (PDF-2, card no 65-0414). It means that the characteristic temperature of the martensitic transformations occurs below the room temperature. On the top of the NiTi alloy the thin layer formed from titanium nitride was identified (PDF-2, card no 65-0565). Lowering value of the incident angle, in GIXD technique, lowered a depth of the X-ray beam penetration. In consequence of that, the intensity ratio of the diffraction lines: TiN and the B2 phase increased. On the other hand, the intensity of diffraction lines belonging to the B2 phase become lower. Simultaneously, intensity of diffraction lines belonging to the TiN got stronger. Quantity of titanium nitride phase increased with decreasing of penetration depth. This fact is evidence of TiN layer formation on the surface of the NiTi alloy.

It is worthy to notice that apart from previously identified diffraction lines (belonging to these two identified phases) there were no additional lines. Especially lines, which could be an evidence of presence of equilibrium phases present in phase equilibrium diagrams Ni-Ti, Ti-N or Ni-N. This fact confirm, that applied procedure did not decompose the B2 parent phase.

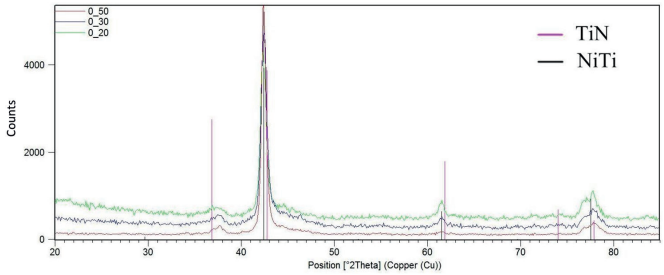

Fig. 1. The GIXD patterns measured at incidence angle of 0.2, 0.3 and 0.50 for layer deposited at 300°C for 30 min

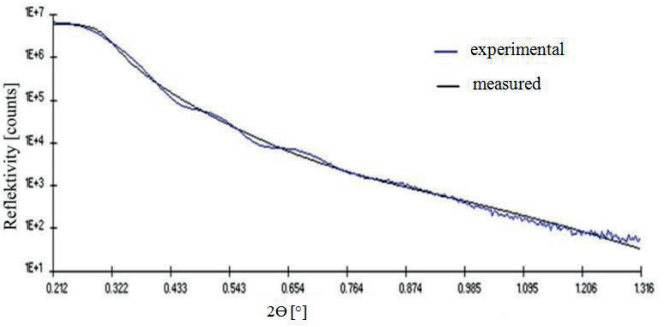

Fig. 2. The reflectivity curve (measured and experimental) for the nitrided layer deposited at 300°C for 30 min

The thickness, surface roughness, interface roughness and density of the nitride layers and NiTi matrix were calculated from X-ray reflectivity curves. An example of the reflectivity curve measured for NiTi nitrided at 300°C for 30 min is shown in Figure 2. Calculated values of thickness, surface roughness and layer density are compared in Table 1. Application of lower deposition temperature and shorter deposition time resulted in forming thinner TiN layer with thickness of about 35 nm. Increase of the nitriding temperature to 300°C and elongation of the deposition time to 30 minutes resulted in increasing of the layer thickness to about 47 nm. Also, application of higher parameters of glow discharge process contributed to reduction in surface roughness of the TiN layer as well as the increase of density calculated for interface between the NiTi alloy and the TiN layer.

TABLE 1

Results obtained from the GIXD and reflectivity measurements.

Parameters of the glow discharge process	Phase	Thickness [nm]	Surface roughness [nm]	Density [g cm^{-3}]
250°C/15min.	NiTi	-	12,4	5,21
	TiN	34,5	10,5	4,06
300°C/30min.	NiTi	-	16,9	5,69
	TiN	46,9	4,1	4,34

The hardness and elastic properties of the nitrided layers were studied with use of nanoindentation method. Changes in hardness and Young's modulus versus increasing of indenter penetration depth are shown in Figure 3 and Figure 4, respectively. Obtained results showed that the TiN layer has a higher hardness and a higher Young's modulus in comparison to the substrate – parent phase B2.

The highest values of parameters achieved for the TiN layer, where the hardness revealed about 7 GPa, and Young's modulus about 60 GPa. With increasing distance from the surface, these values have been reduced. The significant decrease in value of both calculated parameters was observed up to penetration depth of 50 nm. This value is in a good correlation to that calculated from reflectivity measurements (Table 1). It was found that for the parent phase - NiTi substrate, the hardness reached 3 GPa whereas the Young's modulus - 30 GPa.

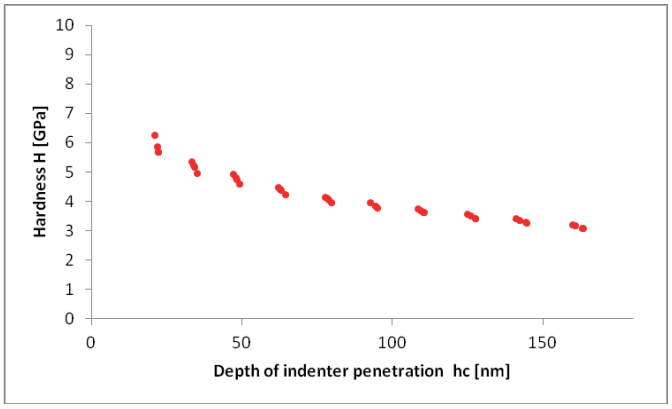

Fig. 3. Change of hardness versus increase of indenter penetration depth measured for the sample nitrided at 300°C for 30 minutes

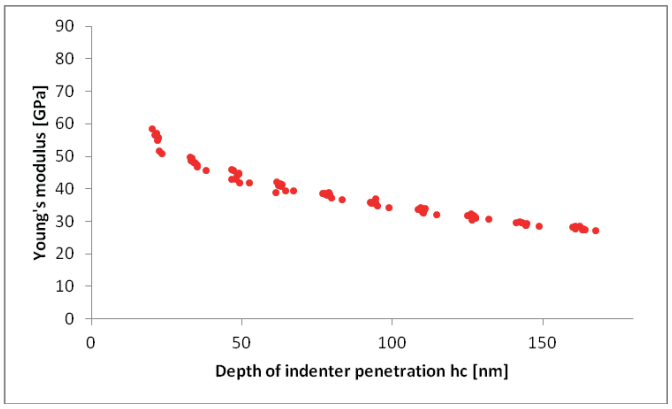

Fig. 4. Change of Young's modulus versus increase of indenter penetration depth measured for the sample nitrided at 300°C for 30 minutes

NiTi alloy after deposition of the hydroxyapatite layers on the nitrided layer

The samples of the NiTi alloy with formed titanium nitride layers have been immersed in simulated body fluid – Hank's solution for 7 days. The hydroxyapatite deposition was carried out at room temperature. Phase identification of the formed multi-layers was carried out basing on the X-ray diffraction patterns measured with use of GIXD technique (Fig. 5). In addition to the previously identified phases (B2-NiTi and TiN), the analysis confirmed the presence of hydroxyapatite (PDF-2, card no. 34-0010) as well as NaCl (PDF-2, card no. 77-2064).

a)

b)

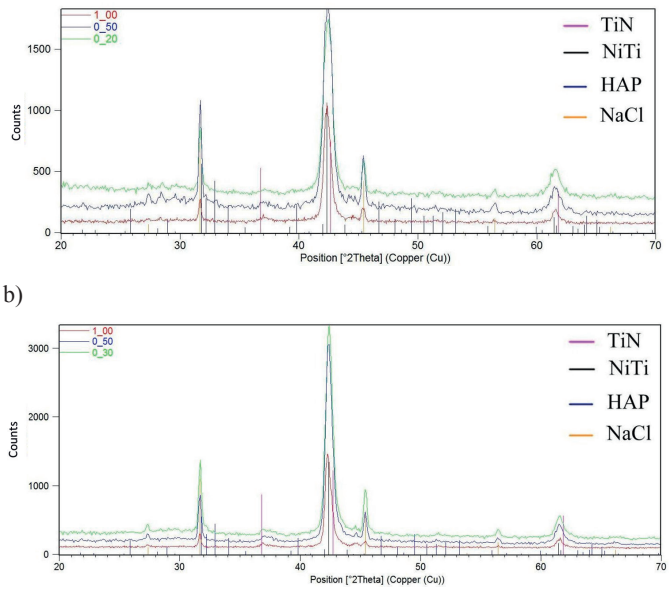

Fig. 5. Phases identification done for GIXD patterns measured at incidence angle of 0.3, 0.5 and 1° for the NiTi alloy nitrided at 250°C/15min (a) and 300°C/30min (b) after deposition of hydroxyapatite layer

The distribution of the deposited hydroxyapatite particles were observed using a scanning electron microscope. Figure 6 shows SEM images observed for NiTi alloy nitrided at 250°C/15min (a) and 300°C/30min (b) coated with the HAp layer. In the case of nitrided alloy under conditions: 250°C/15min, the hydroxyapatite particles revealed homogenous distribution on the nitrided surface in comparison to the sample nitrided under 300°C/30min. This difference may results from the quality of the nitrided surface layer. Results obtained from the reflectivity measurements (Table 1) showed that the surface roughness of TiN layer is higher for lower parameters of the nitriding process. Moreover, deposition with this condition leaded to lowering of TiN density. It means that application of nitriding conditions 250°C/15min structure of the TiN layer is better developed and porous. Such circumstances may be a source for creation of more favorable conditions for homogenous distribution of the hydroxyapatite particles.

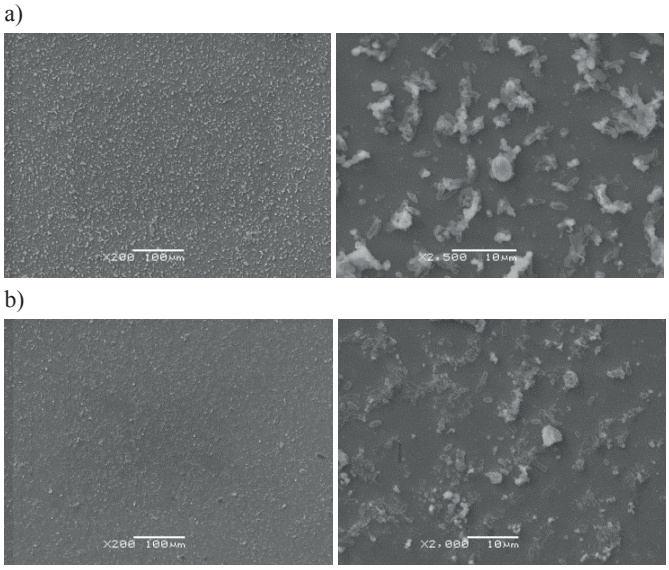

Fig. 6. SEM images observed for NiTi alloy nitrided at 250°C/15min (a) and 300°C/30min (b) coated with the HAp layer

In order to understand the mechanism of hydroxyapatite particles growth, the element distribution maps was determined. The maps of the selected area for chlorine, sodium, phosphorus, calcium and oxygen were measured. Results are shown in Figure 7. HAp particles were round-shaped with average diameters of 2 µm. In these places a higher concentration of elements forming the hydroxyapatite (P, Ca, O) was stated. Apart of that, particle with elongated elliptical shape and a chord length of about 2 µm and 0.5 µm were observed. In these places higher concentration of the Na and Cl was confirmed. It is worthy to notice that the NaCl particles were formed around and under the hydroxyapatite particles. It was confirmed form maps of elements distribution, in which areas of the elements forming hydroxyapatite and NaCl were overlapped. In areas of Na and Cl occurrence, they had weaker contrast, what proved their placement under the HAp particles. Both, the hydroxyapatite and NaCl particles were not deposited directly on the surface of the previously formed titanium nitride layer. First, on the top of the TiN layer, a thin layer consisting mostly of calcium, oxygen and phosphorous (elements which form the basis of the hydroxyapatite particles) was formed. These areas were dominated by the presence of Ca, P and O at the distribution maps of elements (Fig. 7). Furthermore, the broaden diffraction peak appeared in the GIXD patterns measured at incidence angle of 0.3° at the 2θ range from 25° to about 34° 2Θ (Fig. 8). The maximum of this peak is located near the position of the HAp strongest diffraction line (211). These facts suggest that a thin layer consisting mostly from the hydroxyapatite elements is amorphous. Thin amorphous layer was directly formed on the titanium nitride layer and produced the base for the crystallization of the HAp particles.

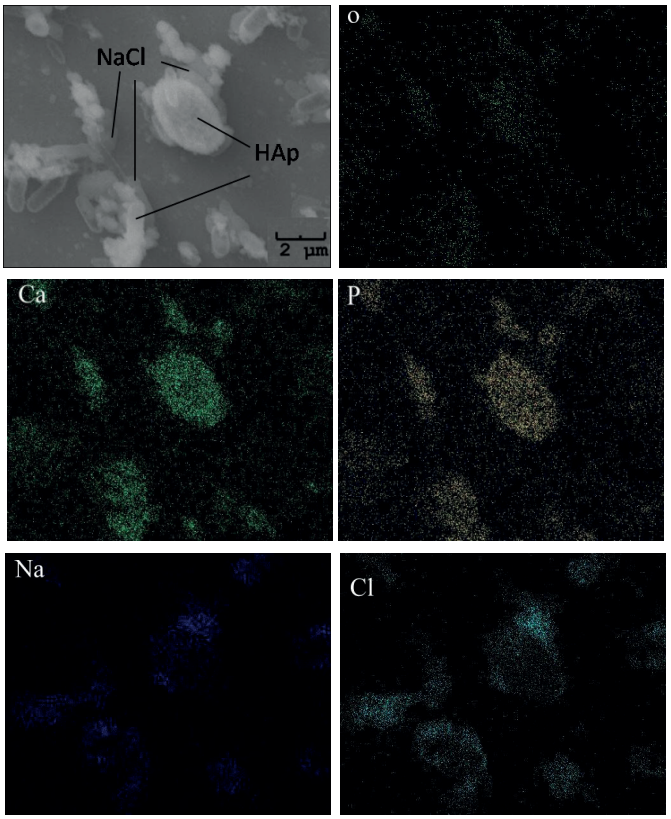

Fig. 7. SEM images and distribution elements maps measured for the NiTi alloy nitrided at 250°C/15min with deposited HAp layer

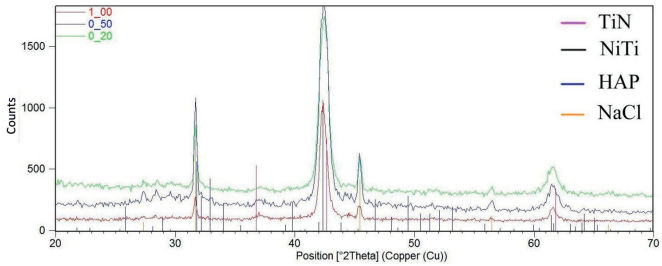

Fig. 8. GIXD patterns measured at incidence angle of 0.3° for the nitrided NiTi alloy with deposited hydroxyapatite layer

4. Summary

The applied deposition processes resulted in obtaining the continuous and homogeneous coatings on the surface of the NiTi alloy. Mainly, the layers were formed from the titanium nitride and hydroxyapatite. The nitriding glow discharge technique carried out at low temperatures (250-300°C) allowed to produce thin titanium nitride layer with its thickness of 35-50 nm. Significant surface development of the titanium nitride layer was observed as a result of the nitriding process at a lower processing parameters (250°C, 15min), which also had contribution in forming of the homogeneous upper layer consisting mainly of hydroxyapatite. These layers were deposited on the surface previously prepared by immersing of the samples in the Hank's solution. The hydroxyapatite crystallized in the form of regularly shaped particles with an average diameter

of about 2 μm. These particles were attached to the surface with a thin layer of amorphous phase consisting mainly of calcium, potassium and oxygen - the elements, which form the hydroxyapatite. Beside the hydroxyapatite particles, the elongated shape sodium chloride particles was formed in the upper layer. Of particular note is the fact, that the glow discharge technique and the hydroxyapatite deposition in the Hank's solution parameters did not lead to decomposition of the NiTi parent phase (B2) to the equilibrium ones.

Acknowledgments

The studies were financially supported from the project N N507 230540 funded by The National Science Centre (NCN).

REFERENCES

[1] T. Yoneyama, S. Miyazaki: Shape memory alloys for biomedical applications. Woodhead Publishing Limited, Cambridge (2009).
[2] L.G. Machado, M. A. Savi, Braz. J. Med. Biol. Res. **36**, 683-691 (2003).
[3] S. Shabalovskaya, J. Anderegg, J. Van Humbeeck, Acta Biomater. **4**, 447–467 (2007).
[4] F. Sun, K. Sask, J.L. Brash, I. Zhitomirsky, Colloid Surface B 67, 132-139 (2008).
[5] X. Liu, P.K. Chu, C. Din, Mater. Sci. **47**, 49–121 (2004).
[6] K. Dudek, B. Szaraniec, J. Lelątko, T. Goryczka, Sol. St. Phen. **203-204**, 90-93 (2013)
[7] S. V. Dorozhkin, Calcium Orthophosphates in Nature, Biology and Medicine. Materials **2**, 399-498 (2009).
[8] Z.D. Cui, H.C. Mana, X.J. Yang, Surf. Coat. Tech. **192**, 347–353 (2005).
[9] A. Dudek, Arch. Metall. Mater. **56,** 1, 135-140 (2011).

Received: 20 October 2014.